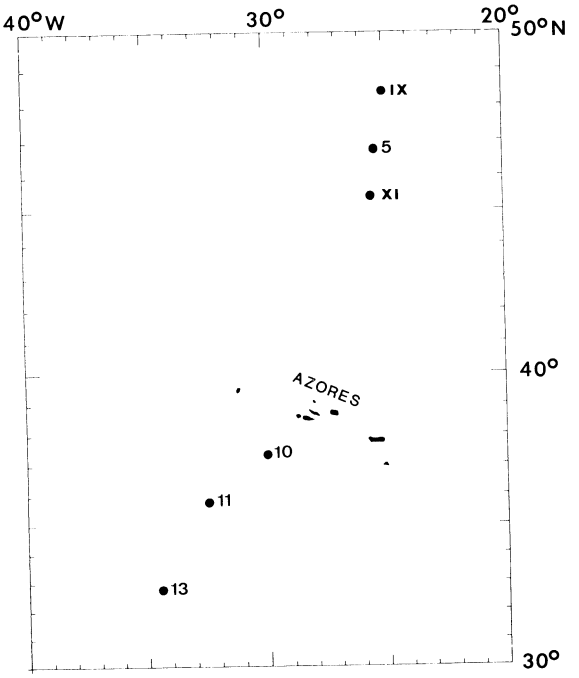

Fig. 1. Location of the box cores from the northeastern Atlantic Ocean discussed in this paper. Arabic numbers refer to box cores taken during APNAP cruise 1986; Roman numbers refer to box cores from APNAP cruise 1988.

We present the results of AMS ^{14}C measurements performed on individual pteropod shells from eastern North Atlantic box cores along a traverse, 32°–48°N. Speculations are made on the relation of aragonite preservation to climatic development in this area during the late Quaternary.

Material and methods

The material described in this paper derives from six box cores taken in the northeastern Atlantic during the 1986 and 1988 APNAP cruises with the *R/V Tyro* (Fig. 1). Core location, water depth and recovery are indicated in Table 1. Preparation of the aragonitic/calcitic shells followed standard procedures (Hut, Ostlund & van der Borg 1986). In a few cases, the sediments directly underlying the pteropod ooze were dated on bulk planktonic foraminiferal material.

TABLE 1. Station location, water depth and core recovery of northeastern Atlantic material discussed in the text

Station	Latitude	Longitude	Depth (m)	Recovery (cm)
T88/9B	48°23′N	25°05′W	3074	28
T86/5B	46°53′N	25°21′W	3121	38
T88/11B	45°24′N	25°26′W	2741	26
T86/10S	37°07′N	30°02′W	2610	36.5
T86/11S	35°44′N	32°33′W	2220	14
T86/13B	32°46′N	34°42′W	2992	17
DANA41953*	41°55′N	32°22′W	100 (water column)	

* The DANA sample refers to pteropod net samples, collected 22/6/1931 at a depth of 100 m in the water column.

TABLE 2. AMS ^{14}C Measurements on material discussed in this paper

Station no.	UtC no.	Position in core (cm)	Type of organism	$\Delta^{13}C$† (‰)	Age BP‡
DANA41953*	1033	100 m (water column)	*Diacria*	2.50	480 ± 50
DANA41953	1034	100 m (water column)	*Diacria*	2.10	370 ± 70
T88/9B	1031	17–18	Pter. fragments	2.03	3690 ± 80
T88/9B	1032	18–19.5	Pter. fragments	1.90	7230 ± 100
T88/9B	1023	**1. 0–2	*Diacria*	1.10	550 ± 60
T88/9B	1027	1. 12–14	Pter. fragments	2.03	3690 ± 80
T88/9B	1024	2. 0–2	*Diacria*	2.40	600 ± 100
T88/9B	1028	2. 12–14	Pter. fragments	2.21	3970 ± 80
T88/9B	1025	3. 0–2	*Diacria*	2.30	1210 ± 60
T88/9B	1029	3. 12–14	Pter. fragments	1.74	4970 ± 70
T88/9B	1026	4. 0–2	*Diacria*	2.40	1870 ± 110
T88/9B	1030	4. 12–14	Pter. fragments	1.67	8020 ± 110
T86/5B	423	1. 0–1	*Diacria*	2.00	510 ± 90
T86/5B	648	1. 0–1	*Diacria*	2.67	790 ± 70
T86/5B	422	1. 0–1	*Diacria*	1.99	770 ± 110
T86/5B	421	2. 0–1	*Diacria*	2.00	1140 ± 90
T86/5B	649	2. 0–1	*Diacria*	2.41	1560 ± 120
T86/5B	418	2. 0–1	*Diacria*	2.00	1210 ± 110
T86/5B	650	2. 0–1	*Diacria*	2.30	1540 ± 80
T86/5B	417	3. 0–1	*Diacria*	2.18	1590 ± 80
T86/5B	416	3. 0–1	*Diacria*	2.00	1740 ± 110
T86/5B	415	4. 0–1	*Diacria*	2.00	1870 ± 90
T86/5B	414	4. 0–1	*Diacria*	2.00	3170 ± 120
T86/5B	699	2–3	Forams	1.87	1210 ± 80
T86/5B	700	3–4	Forams	2.00	2700 ± 80
T86/5B	441	1. 1–2	*Diacria*	2.00	720 ± 110
T86/5B	437	1. 1–2	*Diacria*	1.96	680 ± 110
T86/5B	425	1. 1–2	*Diacria*	2.00	710 ± 80
T86/5B	440	3. 1–2	*Diacria*	2.00	1740 ± 130
T86/5B	439	3. 1–2	*Diacria*	2.00	1710 ± 110
T86/5B	438	3. 1–2	*Diacria*	1.72	1690 ± 90
T86/5B	424	4. 1–2	*Diacria*	2.00	2100 ± 130
T88/11B	1018	1. 0–1	*Diacria*	1.80	230 ± 50
T88/11B	1019	1. 0–1	*Diacria*	2.20	620 ± 90
T88/11B	1020	1. 0–1	*Diacria*	2.00	620 ± 50
T88/11B	1021	3. 0–1	*Diacria*	2.70	1570 ± 60
T88/11B	1022	4. 0–1	*Diacria*	1.80	2130 ± 90
T86/10S	662	0–1	*Diacria*	0.99	−480 ± 90
T86/10S	665	0–1	*Caveolina*	1.89	−190 ± 90
T86/10S	666	0–1	*Clio*	1.85	1070 ± 100
T86/11S	660	1. 0–1	*Diacria*	1.94	32 ± 60
T86/11S	661	3. 0–1	*Diacria*	1.00	690 ± 70
T86/13B	653	1. 0–1	*Diacria*	1.78	10,610 ± 120
T86/13B	654	2. 0–1	*Diacria*	1.14	7160 ± 80
T86/13B	735	3. 0–1	*Diacria*	0.30	8170 ± 180
T86/13B	655	4. 0–1	*Diacria*	1.46	15,600 ± 200
T86/13B	656	5. 0–1	*Diacria*	1.30	14,600 ± 200
T86/13B	657	1. 0–1	*Cuvierina*	1.30	10,170 ± 110
T86/13B	658	2. 0–1	*Cuvierina*	1.59	13,400 ± 300
T86/13B	659	3. 0–1	*Cuvierina*	1.31	14,140 ± 190

*The two DANA samples derive from plankton tows at a depth of 100 m.

**Numbers 1–4 refer to different staining stages of the test of the pteropod species *Diacria trispinosa* and *Cuvierina columnella* (1 = white; 4 = dark brown). The four stages are collected both from the 0–2 as from the 12–14 cm downcore level. Pteropods from the 12–14 cm level are all fragmented.

†$\Delta^{13}C$ values measured at the Geology Department, Utrecht.

‡Age in years Before Present from ^{14}C activity after normalization to $\delta^{13}C = -25‰$. No correction applied for reservoir age.

RESULTS

Table 2 lists all AMS ^{14}C measurements performed on our material. In the table, ages are not corrected for reservoir age. The majority of the samples derives from surface sediments, however, preservation horizons downcore were also taken into account (T88/9B). To determine the nature of the surficial pteropod ooze, a foraminiferal sample from T86/5B directly underlying the ooze was measured. Its generally younger age, compared to most ages of the pteropod ooze specimens, indicates that the ooze is a lag deposit. Preservation of the aragonitic shells is strongly enhanced by the Fe/Mn coating.

In order to compare these ages to terrestrial chronologies from plant material, a correction for reservoir age has to be made. To achieve this, we measured pteropods collected during the DANA Expeditions in 1931 (thus before atomic pollution) in plankton nets at a depth of 100 m. AMS ^{14}C dates on these specimens yielded ages of 370 and 480 B.P. (average of 425 yrs), respectively, which is in good agreement with the theoretical reservoir age model of Stuiver, Pearson and Braziunas (1986). However, strictly speaking, the reservoir age is reserved for pre-industrial samples in contrast with pre-bomb samples. ^{14}C dilution by fossil fuels is in the order of 10‰ (*ca.* 80 yrs) for North Atlantic surface waters (Druffel & Suess 1983; Bard *et al.* 1988). From Figure 3 in Druffel and Suess (1983), it becomes clear that the period after 1930 accounts for the major part of this so-called Suess effect. In the preceding period, dilution is in the order of 2–3‰ (*ca.* 20 yrs). As our specimens were collected in 1931, we decided not to correct for the entire Suess effect, but only for samples collected before 1930. Hence, in the text and figures all our data (from uncorrected data in Table 2) are corrected by −400 years for reservoir age. The corrected ages were cumulatively plotted in three different time frames: 16,000–2000 B.P. (Fig. 2), the last 2000 years (Fig. 3), and the period A.D. 1500–1900 (Fig. 4). The implications of the plots are discussed below.

DISCUSSION — PTEROPOD PRESERVATION IN RELATION TO CHANGING CLIMATE

From our data set, it becomes clear that aragonite preservation is a recurrent feature during the last 16,000 years in the eastern North Atlantic. Figure 2 shows that, on a longer time scale, preservation periods occurred from 15,200–13,000, 10,300–9700, 8000–6000 and 4500–2700 B.P. The first two events correspond to Termination 1A and 1B, respectively (*cf.* Bard *et al.* 1987); a worldwide preservation peak centered around 14,000 B.P. has also been postulated by Berger (1977). The

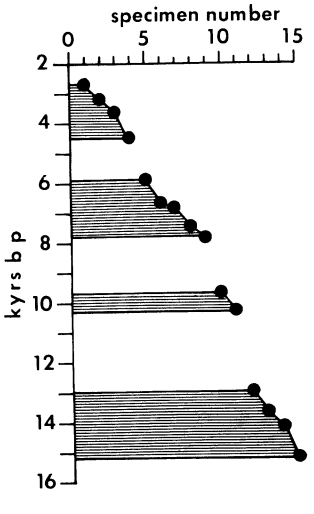

Fig. 2. Cumulative plot of 15 pteropod specimens *vs.* time (16,000–2000 B.P.). ^{14}C ages corrected for reservoir age by −400 years. Shaded areas indicate periods of aragonite preservation.

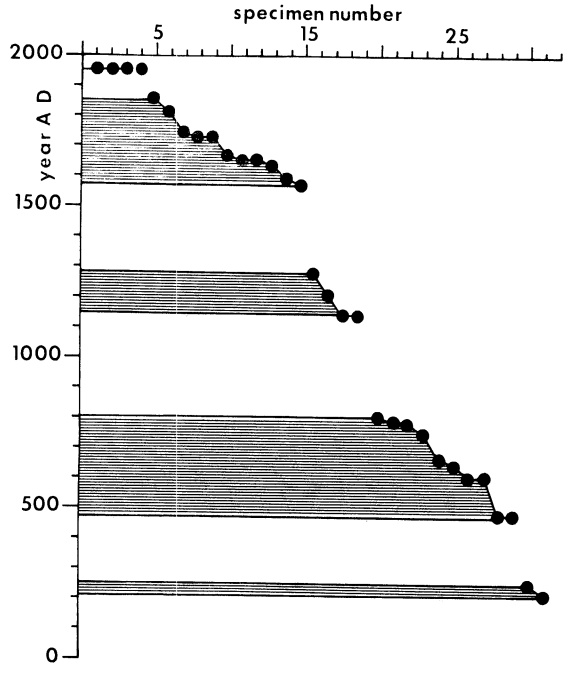

Fig. 3. Cumulative plot of 31 pteropod specimens *vs.* time (the last 2000 years). ^{14}C ages corrected for reservoir age by −400 years. Shaded areas indicate periods of aragonite preservation.

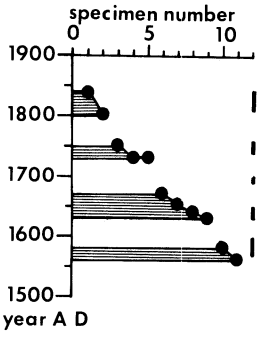

Fig. 4. Cumulative plot of 11 pteropod specimens *vs.* time (the Little Ice Age). ^{14}C ages corrected for reservoir age by −400 years. Shaded areas indicate periods of aragonite preservation. Vertical bars mark the cold periods as established by Serre-Bachet and Guiot (1987).

third period approximates Termination 1C (Berger 1990); Kassens & Sarnthein (1989) mention enhanced aragonite preservation around 7000 B.P. in the equatorial Atlantic. The first three preservation spikes are thus strongly correlated to the deglaciation steps following the last glacial maximum. Also, for the period 4500–2700 B.P., a link to climate fluctuations can be made considering major climatic changes at about 4200, 3600 and 2500 B.P. reported by Frenzel (1975).

On a limited time scale (Fig. 3), distinct intervals of aragonite preservation can be observed from A.D. 200–250, 480–800, 1150–1180, 1560–1840 and Recent. The period, A.D. 1560–1840, nicely matches the Little Ice Age, which is characterized by various cold spells between 1570 and 1840 (Serre-Bachet & Guiot 1987). The work of these authors is based on reconstructions of the mean summer temperature by tree-ring densitrometric measurements from the Alps and the Mediterranean region. Plotting our data from this period in an even narrower time frame (Fig. 4), periods of pteropod preservation show a remarkable fit with the cold periods established by Serre-Bachet & Guiot (1987), *i.e.*, A.D. 1570–1600, 1630–1650, 1690–1700, 1740–1760 and 1810–1840,

although we are aware that, considering the accuracy of the ^{14}C technique and the corrections applied for the reservoir age, a little wishful thinking cannot be excluded.

CONCLUSION

In summary, conditions leading up to pteropod preservation prevailed during intervals of climatic change, such as the Last Glacial/Holocene transition, the period 4500–2700 B.P. and the Little Ice Age. We conclude that other intervals of aragonite preservation within the last 2000 years also may have been caused by similar short-term periods of climatic change.

ACKNOWLEDGMENTS

Cruises Tyro 1986/88 were financed by the Dutch Council of Sea Research (SOZ). The manuscript greatly benefitted from critical remarks and helpful suggestions by W. H. Berger and an anonymous reviewer.

REFERENCES

Bard, E. 1988 Correction of accelerator mass spectrometry ^{14}C ages measured in planktonic foraminifera: paleoceanographic implications. *Paleoceanography* 3(6): 635–645.

Bard, E., Arnold, M., Maurice, P., Duprat, J., Moyes, J. and Duplessy, J.-C. 1987 Retreat velocity of the North Atlantic polar front during the last deglaciation determined by ^{14}C accelerator mass spectrometry. *Nature* 328: 791–794.

Berger, W.H. 1977 Deep-sea carbonate and the deglaciation preservation spike in pteropods and foraminifera. *Nature* 269: 301–304.

_____1978 Deep-sea carbonate: pteropod distribution and the aragonite compensation depth. *Deep Sea Research* 25(5): 447–452.

_____1990 The Younger Dryas cold spell – a search for causes. *Global and Planetary Change* 89(3): 219–237.

Berner, R. A. 1977 Sedimentation and dissolution of pteropods in the ocean. *In* Andersen, N. R. and Malahoff, A., eds., *The Fate of Fossil Fuel CO_2 in the Oceans.* New York, Plenum Press: 323–343.

Frenzel, B. 1975 The distribution pattern of Holocene climatic change in the Northern Hemisphere. *In* Lamb, H., convener, Proceedings of the *WMO/IAMAP Symposium on Long-Term Climatic Fluctuations.* Geneva, World Meteorological Organization: 105–118.

Ganssen, G. M. and Lutze, G. F. 1982 The aragonite compensation depth at the northeastern Atlantic continental margin. *"Meteor" Forschungsergeb* C36: 57–59.

Hut, G., Ostlund, H. G. and van der Borg, K. 1986 Fast and complete CO2-to-graphite conversion for ^{14}C Accelerator Mass Spectrometry. *In* Stuiver, M. and Kra, R. S., eds, Proceedings of the 12th International ^{14}C Conference. *Radiocarbon* 28(2A): 186–190.

Kassens, H. and Sarnthein, M. 1989 A link between paleoceanography, early diagenetic cementation and shear strength maxima in Late Quaternary sediments? *Paleoceanography* 4(3): 253–269.

Melkert, M. J., Ganssen, G. M., Helder, W. and Troelstra, S. R., in press, Episodic preservation of pteropod oozes in the deep N. E. Atlantic Ocean: Climatic changes and hydrothermal activity. *Marine Geology.*

Price, B. A., Killingley, J. S. and Berger, W. H. 1985 On the pteropod pavement of the eastern Rio Grande Rise. *Marine Geology* 64: 217–235.

Serre-Bachet, F. and Guiot J. 1987 Summer temperature changes from tree-rings in the Mediterranean area during the last 800 years. *In* Berger, W. H. and Labeyrie, L. D., eds, *Abrupt Climate Change.* Dordrecht, The Netherlands, D. Reidel: 89–97.

Stuiver, M., Pearson, G. W. and Braziunas, T. 1986 Radiocarbon age calibration of marine samples back to 9000 cal yr BP. *In* Stuiver, M. and Kra, R. S., eds, Proceedings of the 12th International ^{14}C Conference. *Radiocarbon* 28(2B): 980–1021.

Troelstra, S. R., Ganssen, G. M., Sennema, E. J., Klaver, G. Th., Alderliesten, C., van der Borg, K. and de Jong, A. M. F. 1987 Late Quaternary stratigraphy and sedimentology of the central North Atlantic: A progress report. *Nuclear Instruments and Methods* B29: 317–321.

[RADIOCARBON, VOL. 33, NO. 3, 1991, P. 283–289]

SHELL HASH DATING AND MIXING MODELS FOR PALIMPSEST MARINE SEDIMENTS

PETER S. ROY

Department of Minerals and Energy, Geological Survey of New South Wales and
Department of Geography, The University of Sydney, NSW 2006, Australia

ABSTRACT. The dating of palimpsest marine sediments using broken shell fragments (shell hash) is considered to be a necessary but unreliable technique because of the mixed age of the fragments. An analysis of geological mixing models and radiocarbon data on shell hash from sandy sediments on the southeast Australian coast and shelf are used to examine the possibility for simulating the depositional processes, and thus, to better understand the age structure of the deposits.

INTRODUCTION

Classic mixing models devised for sediments accumulating in the deep sea and on allochthonous shelves (Berger & Heath 1968; Guinasso & Schink 1975; Carney 1981) are not readily applicable to wave-dominated environments with palimpsest sediments, such as the southeast Australian shelf. Here, sediment transporting and reworking mechanisms are likely to be "episodic," in the sense used by Dott (1983); mixing rates almost everywhere are very much greater than accumulation rates (which, in some cases, are negative), and contemporary sediment sources, sinks and transport pathways are poorly defined. Thus, it is difficult to apply conventional theories of mixing and strata formation as, *e.g.*, in the Washington Shelf study by Nittrouer and Sternberg (1981).

Late Quaternary sediments in coastal and nearshore environments in southeast Australia are composed, in large part, of marine sands – mainly quartz and biogenic carbonate. The carbonate is made up of broken fragments (the tests of marine organisms), and has been extensively dated by ^{14}C methods to determine the time of deposition of the enclosing sediment (Thom, Polach & Bowman 1978; Thom *et al.* 1981; Chapman *et al.* 1982; Thom 1984). This material is not used by preference, but because nothing else of a more *in-situ* nature is available. Commonly, the samples submitted for dating are made up of hundreds of biogenic carbonate fragments (shell hash), each presumably with a different age and history of reworking and transport – an extreme case of the stratigraphic disordering described by Flessa, Cutler & Meldahl (1989). Clearly, the reported age is some average figure that cannot precisely correspond to the time the enclosing sediment was deposited. That bulk ^{14}C samples are made up of an admixture of different-aged shell fragments has recently been confirmed by Walbran *et al.* (1989), who used accelerator mass spectrometer (AMS) techniques to date individual fragments of *Acanthaster planci* in sediment cores from the Great Barrier Reef. Figure 1 shows the relationship between the ^{14}C date on bulk carbonate sand and the AMS ages for individual grains located close by. If the carbonate sand has the same age structure as the AMS samples, then bulk ^{14}C dates represent a strongly skewed spread of individual ages that cluster within 400 years of the reported age, but include a proportion that are considerably older. Other indications that reported ^{14}C dates on bulk shell samples are distorted (age-shifted) come from presently active depositional surfaces that return shell hash ages of 1000–2000 years B.P. Nielsen and Roy (1982) discussed this mixing phenomenon and attempted, with partial success, to calculate a correction factor to compensate for the incorporation of old shell.

Despite this mixing problem, the broad patterns shown by hundreds of ^{14}C dates from a number of Holocene depositional environments in southeast Australia show sensible trends. Patterns of deposition fit geological models of how, *e.g.*, coastal sand barriers and estuarine flood-tide deltas form (Fig. 2), and dated sequences in cores rarely display the stratigraphic disorder described by

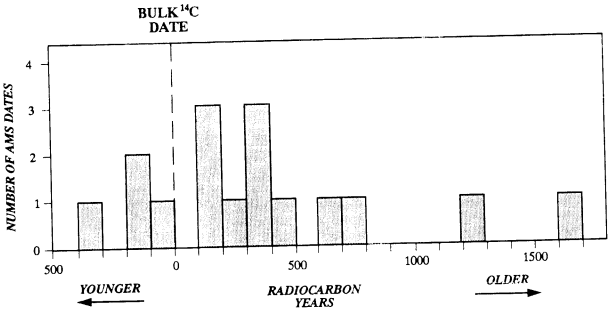

Fig. 1. Histogram showing discrepancies between ^{14}C ages of bulk carbonate sand samples (in three cores) and AMS dates on individual fragments of *Acanthaster planci* in the sand. All AMS samples are within 15 cm of the bulk samples, and average sedimentation rates in the cores are in the order of 1.0–2.0 mm yr^{-1}. Based on data from the Great Barrier Reef in Walbran *et al.* (1989).

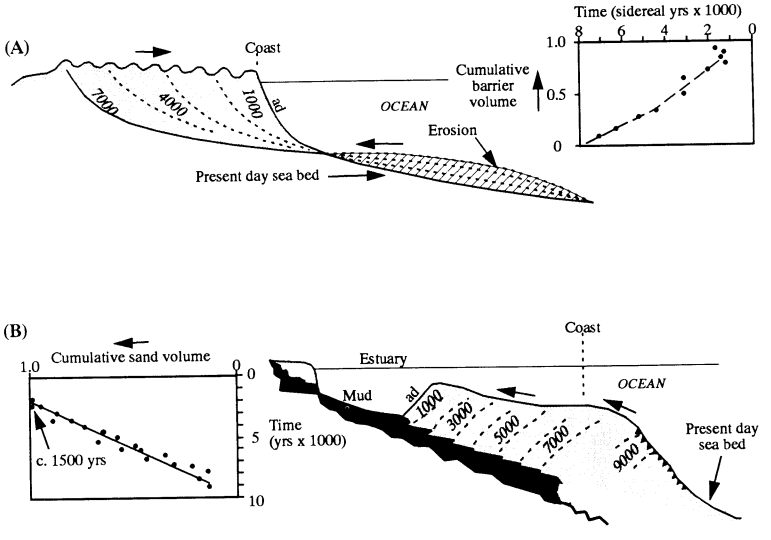

Fig. 2. Diagrammatic cross-sections of sandy coastal depositional sequences: (A) prograded barrier and (B) estuarine flood-tide delta, both with presently active depositional surfaces (ad); arrows show directions of sediment supply and progradation. In each environment, ^{14}C-dated shell-hash samples (•) document regular patterns of volumetric change. Based on data from the Tuncurry barrier (Chapman *et al.* 1982) and the Port Hacking tidal delta (Roy 1984).

Flessa, Cutler and Meldahl (1989) and Cutler and Flessa (1990). Is it possible to improve our understanding of late Quaternary depositional processes by unraveling the mixing problem? The following is a preliminary attempt to devise a model that describes physical mixing of shell fragments in sandy sediments on a moderately high-energy coast that is undergoing extensive reworking.

THE MIXING MODEL

If a single shell dies and is immediately buried by accumulating sediment, its ^{14}C age (corrected to sidereal years) should indicate the time of deposition of the enclosing sediment layer. In coastal

and shelf depositional environments, the closest approach to these passive conditions is in deep estuarine basins, where mud slowly settles from suspension, and buries shells living and dying on the bed of the estuary. But even here, biological activity exists and, given the slow rates of sedimentation (0.1–0.5 m yr^{-1}, according to Roy (1984)), there is a good chance that the test will be bioturbated upwards or downwards into younger or older sediment layers (Roy & Crawford 1984). In these types of settings, the mixing mechanisms are quite well understood (Carney 1981); mixing depths have been measured using radioactive tracers (Carpenter, Peterson & Bennett 1985), and the processes have been successfully modeled (Wheatcroft *et al.* 1990). In higher energy environments, such as beaches, shorefaces, tidal inlets and the inner shelf, physical reworking by waves and currents, as well as by biological processes, ensures an even greater degree of mixing. Here, factors such as episodicity and event magnitude, recurrence interval, recovery time and preservation potential (Dott 1983) are poorly understood, and limit our ability to apply conventional mixing models.

The elements of the geological mixing model proposed here are:

1. Periodic disturbance of the sea bed to variable depths and at various frequencies, creating a near-surface zone of reworking or mixing in the sediment pile
2. Progressive addition of the tests of newly dead organisms (contemporary shell) to the sea bed at a semiconstant rate over geological time spans
3. A slow but constant rate of breakdown of older shell in the zone of reworking due to abrasion, decay, *etc.*
4. Addition or subtraction of clastic sediment (deposition or erosion) that shifts the zone of reworking upwards or downwards through the sediment pile
5. Addition of old shell fragments eroded from elsewhere and transported to a new site of deposition.

Mixing in the reworked zone occurs during storms, as sand waves and ripples migrate over the sea bed, and during quiet periods, by bioturbation. Geological studies by Hudson and Roy (1988) show that the depth of reworking on the open coast decreases offshore with increasing water depth. Depths range from many meters on the beach face to 20 cm or so on the mid-shelf. Since deep reworking can be expected to occur much less frequently than shallow reworking, it is likely that the long-term mixing process can be expressed as some type of exponential function (inset in Fig. 3), the actual values and shape of which are site-specific. This concept is similar to the multiple mixed layers mentioned by Nittrouer and Sternberg (1981: Figs. 14, 15).

Three mixing scenarios of increasing complexity are considered below:

Model A. In-situ reworking with addition of no new sediment except for contemporary shell

Model B (1). In-situ reworking as in Model A with addition of new sediment (but containing no old shell) at a constant rate

Model B (2). In-situ reworking as in Model B (1) accompanied by slow erosion of the sea bed

Model C. Same depositional scenario as for Model B, but with the addition of old shell hash derived from elsewhere.

Model A is illustrated in Figure 3 by a vertical segment into the sea bed, which also represents a graph showing the relative proportions of different-aged shell hash in the reworked zone. At time t_1, the parent sediment, 2000 years old, has been reworked to depth 'd', and a proportion of younger shell averaging 1000 years old has been added. Although, in reality, the younger shell

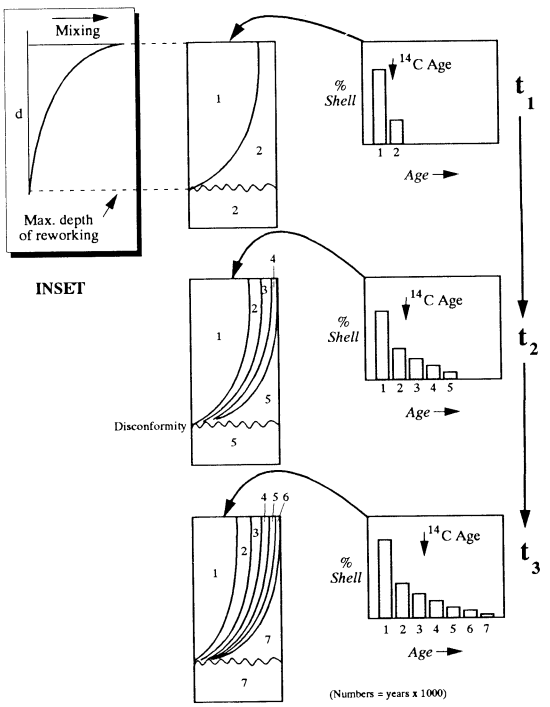

Fig. 3. Mixing Model A shows *in-situ* reworking of parent sediment to depth 'd', below the sea bed and the progressive addition of contemporary shell (averaging 1000 yrs old). The inset depicts a hypothetical mixing function that defines the depth of reworking and the vertical distribution of young shell in the mixed zone. The parent sediment is assumed to be 2000 years old at time t_1, and 7000 years old at t_3, 5000 years later. Histograms at each time step indicate the relative proportions of various-aged shell fragments on the contemporary sea bed. Note that the measured ^{14}C age of the sea bed becomes progressively older (age-shifted) because of upward mixing of old shell.

fragments are distributed throughout the reworked zone, the mixing function predicts that most will occur in its upper part, and least near its base. The relative proportions are indicated by a concentration profile in Figure 3, time t_1.

At times, t_2 and t_3, 3000 and 5000 years later (Fig. 3), progressive mixing can be depicted figuratively as successive increments of younger and younger shell. Since the amount of old shell is expected to decrease with time due to abrasion, decay, *etc.*, the "slices" representing older shell proportions in Figures 3 and 4 are thinner than for younger shell. A disconformity is soon created at the base of the reworked zone. The overall effect is that the surface sediments appear older than the contemporary age of the sea bed, whereas the sediment within the reworked zone appears younger than the parent sediment. Figure 4 illustrates other effects of *in-situ* reworking. An age structure is created within the mixed zone that becomes older downwards and, despite the original age of the parent sediment, has ^{14}C ages that are confined to mid- to late Holocene. A similar trend to that shown in Figure 4 could also be expected if the sea bed was slowly eroding rather than static (Model B (2)).

Thus, *in-situ* reworking is an alternative explanation of what normally would be viewed as slow upward accretion under postglacial stillstand conditions. The age pattern shown in Figure 4 has been noted in regard to the inner shelf sand sheet in southeast Australia (Colwell & Roy 1983;

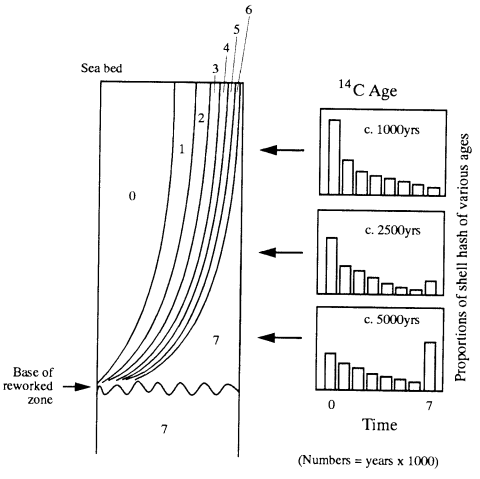

Fig. 4. Illustration of the way in which a regular age structure (age increasing downwards) can be created by *in-situ* reworking of a parent sediment 7000 years old. With, say 26,000-year-old parent sediment, this trend is similar and the ^{14}C ages only slightly older. It is speculated that the relative proportions of the various aged added-shell fractions would progressively decrease from 0–7 (7000) years.

Thom & Roy 1985) and also on the upper surface of the shelf sand bodies off the south Sydney coast (Roy 1985).

In Model B (1), deposition is superimposed on *in-situ* reworking (Model A), but without the introduction of old shell hash. Figure 5A shows four, 1000-year time steps in which the zone of reworking is progressively raised upwards as sediment accumulates. Unlike Model A, a disconformity does not form in this sediment sequence, nor do surface sediments become progressively older with time. The faster the sedimentation rate, the closer the measured ^{14}C age of the sea bed approaches its contemporary age (*i.e.*, zero). Figure 5B illustrates how dependent the ^{14}C age of a shell-hash sample is on the proportions of different-aged shell fractions. Because of the decay of radioactive ^{14}C, the contribution by older shell to the measured ^{14}C age is much less than that of more recent shell. For layer 'x', in the subsurface, it is interesting to note that mixing causes its real age (shown in brackets in Fig. 5A) to be underestimated by ^{14}C dating. The discrepancy increases with time even though the layer is not being actively reworked during later time steps t_3 and t_4.

For slower sedimentation rates, the discrepancy between true and measured ages in the subsurface becomes larger, and is presumably a maximum for *in-situ* reworking with no added sediment). Conversely, for shallower depths of reworking, such as would be expected under quieter conditions in deeper water, the discrepancy between true and measured ages decreases, even though the rate of sedimentation remains unchanged.

Figure 6 shows apparent ages of surface sediments collected in various water depths off Sydney. Although there is some scatter, the trend of increasing age with increasing depth is what would be predicted if sedimentation rates decreased, and *in-situ* reworking becomes more intense as the offshore sea bed deepens. This accords with what is known about the geological setting (Roy 1984), but other variables, such as depth and intensity of reworking and age of parent sediments, probably also play a role.

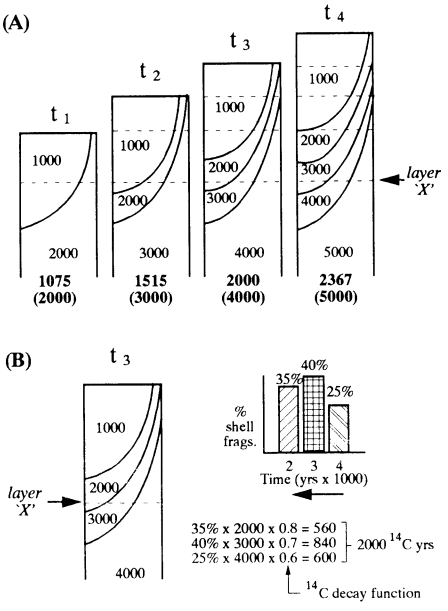

Fig. 5. Mixing Model B showing: (A) progressive sedimentation at four 1000-year time steps. Accretion causes the zone of reworking to move upwards, and no disconformity forms in the sediment pile. Using the method described in (B), below, ^{14}C ages of shell hash in layer "x" are calculated at each time step (age of parent sediment in brackets); (B) a method for determining the ^{14}C age of shell hash in layer "x" (at time t_3), given that the proportions of the various-aged shell fractions are known. The ^{14}C decay function is only approximate.

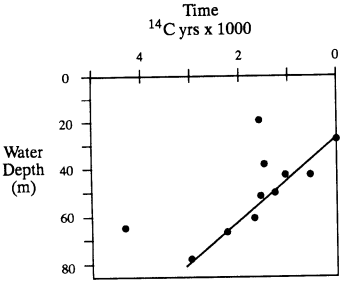

Fig. 6. Radiocarbon ages of shell hash in surface sediments, sampled with a small pipe dredge offshore from Sydney, show a tendency to increase with increasing water depth (from Roy 1985).

In a depositional (accreting) sedimentary environment, if old shell fragments are added to the sea bed and mixed downwards with contemporary shell hash, the overall age of the reworked zone will become older. This is the situation for Model C, which has not yet been simulated. Interestingly, the addition of old shell in Model C reduces the discrepancy predicted in Model B (1) between the actual time of deposition and the measured ^{14}C age of the biogenic material. This exemplifies the complexities created by mixing of materials from diverse sources, and highlights the challenge of simulating "real" conditions as described in Model C.

CONCLUSIONS

With growing sophistication of the various radiometric dating technologies, there is heightened awareness of the range of likely errors that can influence age determinations. However, it seems that the chemical factors leading to dating errors are better understood by analytical laboratories than are the physical environmental factors that are the concern of the field scientist. The theoretical models presented here are a tentative first step towards better understanding physical mixing in sandy sediments. Underlying assumptions need to be refined and quantified, but clearly,

the approach is amenable to computer simulation (*e.g.*, Cutler & Flessa 1990). There may also be applications to other techniques of dating such as thermoluminescence (TL). Future lines of research may include cross-calibration of ^{14}C dates against other measurements (*e.g.*, TL and electron spin resonance (ESR)), but direct measurements of individual shell fragments by AMS is not considered to be a practical approach at this time, because of the cost of dating very large numbers of samples.

ACKNOWLEDGMENTS

The ideas expressed in this paper were presented at a Quaternary Dating Workshop held in Canberra, Australia in October 1990. The support and helpful comments of Richard Gillespie, Alan Cutler and Karl Flessa are greatly appreciated.

REFERENCES

Berger, W. H. and Heath, G. R. 1968 Vertical mixing in pelagic sediments. *Journal of Marine Research* 26: 134-143.

Carney, R. S. 1981 Bioturbation and biodeposition. *In* Boucot, A. J., ed., *Principles of Benthic Marine Paleoecology*. New York, Academic Press: 843-845.

Carpenter, R., Peterson, M. L. and Bennett, J. T. 1985 ^{210}Pb-derived sediment accumulation and mixing rates for the greater Puget Sound region. *Marine Geology* 64: 291-312.

Chapman, D. M., Geary, M., Roy, P. S. and Thom, B. G. 1982 *Coastal Evolution and Coastal Erosion in New South Wales*. Sydney, Coastal Council of New South Wales: 341 p.

Colwell, J. B. and Roy, P. S. 1983 Description of subsurface sediments from the east Australian continental shelf (Sonne Cruise S0-15). *Bureau of Mineral Resources Record* 83/21: 66 p.

Cutler, A. H. and Flessa, K. W. 1990 Fossils out of sequence: Computer simulations and strategies for dealing with stratigraphic disorder. *Palaios* 5: 227-235.

Dott, R. H, Jr. 1983 1982 SEPM presidential address: Episodic sedimentation - how normal is average? How rare is rare? Does it matter? *Journal of Sedimentary Petrology* 53: 5-23.

Flessa, K. W., Cutler, A. H. and Meldahl, K. H. 1989 Taphonamic processes and stratigraphic disorder. *Abstracts, 28th International Geological Congress*: 1.493-1.494.

Guinasso, N. L. and Schink, D. R. 1975 Quantitative estimate of biological mixing rates in abyssal sediments. *Journal of Geophysical Research* 80: 3032-3043.

Hudson, J. P. and Roy, P. S. 1988 Seabed mobility in south-eastern Australia - the Narrabeen Beach embayment. *Coastal Studies Report*, December: 32 p.

Nielsen, A. F. and Roy, P. S. 1982 Age contamination of radiocarbon dates on shell hash from coastal sand deposits: SE Australian examples. *Proceedings of the 5th Australian Conference on Coastal and Ocean Engineering*: 177-182.

Nittrouer, C. A. and Sternberg, R. W. 1981 The formation of sedimentary strata in an allochthonous shelf environment: the Washington Continental Shelf. *Marine Geology* 42: 201-232.

Roy, P. S. 1984 Holocene sedimentation histories of estuaries in southeastern Australia. In *Estuarine Environments of the Southern Hemisphere*. Department of Conservation and Environment, Perth, Western Australia. *Bulletin* 161: 2-60.

_____1985 Marine sand bodies on the south Sydney shelf, S.E. Australia. *Coastal Studies Unit Technical Report* 85/1. Department of Geography, The University of Sydney, Australia: 262 p.

Roy, P. S. and Crawford, E. A. 1984 Heavy metals in a contaminated Australian estuary - dispersion and accumulation trend. *Estuarine, Coastal and Shelf Science* 19: 41-58.

Thom, B. G. 1983 Transgressive and regressive stratigraphies of coastal sand barriers in southeastern Australia. *Marine Geology* 56: 17-158.

Thom, B. G., Bowman, G. M., Gillespie, R., Temple, R. and Barbetti, M. 1981 *Radiocarbon Dating of Holocene Beach Ridge Sequences in Southeast Australia*. Department of Geography, University of New South Wales, Duntroon. *Monograph* 11: 36 p.

Thom, B. G., Polach, H. and Bowman, G. (ms.) 1978 Holocene Age Structure of Coastal Sand Barriers in NSW, Australia. Department of Geography, University of New South Wales, Duntroon. Unpublished report: 86 p.

Thom, B. G. and Roy, P. S. 1985 Relative sea levels and coastal sedimentation in southeast Australia in the Holocene, *Journal of Sedimentary Petrology* 55: 257-264.

Walbran, P. D., Henderson, R. A., Jull, A. J. T. and Head, M. J. 1989 Evidence from sediment of long-term *Acanthaster planci* predation on corals of the Great Barrier Reef. *Science* 245: 847-850.

Wheatcroft, R. A., Jumars, P. A., Smith, C. R. and Nowell, R. M. 1990 A mechanistic view of the particulate biodiffusion coefficients: Step lengths, rest periods and transport directions. *Journal of Marine Research* 48: 177-207.